

2004

Initial thermal design of microchannel heat sink for low-orbit micro-satelites [i.e., satellites]

Amaury Jean Henri Heresztyn
San Jose State University

Follow this and additional works at: https://scholarworks.sjsu.edu/etd_theses

Recommended Citation

Heresztyn, Amaury Jean Henri, "Initial thermal design of microchannel heat sink for low-orbit micro-satelites [i.e., satellites]" (2004). *Master's Theses*. 2661.

DOI: <https://doi.org/10.31979/etd.rq58-3qet>

https://scholarworks.sjsu.edu/etd_theses/2661

This Thesis is brought to you for free and open access by the Master's Theses and Graduate Research at SJSU ScholarWorks. It has been accepted for inclusion in Master's Theses by an authorized administrator of SJSU ScholarWorks. For more information, please contact scholarworks@sjsu.edu.

**INITIAL THERMAL DESIGN OF MICROCHANNEL HEAT SINK
FOR LOW-ORBIT MICRO-SATELITES**

A Thesis

Presented to

The Faculty of the Department of
Mechanical and Aerospace Engineering
San Jose State University

In Partial Fulfillment

of the Requirements for the Degree

Master of Science

By

Amaury Jean Henri Heresztyn

December 2004

UMI Number: 1425463

Copyright 2004 by
Heresztyn, Amaury Jean Henri

All rights reserved.

INFORMATION TO USERS

The quality of this reproduction is dependent upon the quality of the copy submitted. Broken or indistinct print, colored or poor quality illustrations and photographs, print bleed-through, substandard margins, and improper alignment can adversely affect reproduction.

In the unlikely event that the author did not send a complete manuscript and there are missing pages, these will be noted. Also, if unauthorized copyright material had to be removed, a note will indicate the deletion.

UMI[®]

UMI Microform 1425463

Copyright 2005 by ProQuest Information and Learning Company.

All rights reserved. This microform edition is protected against
unauthorized copying under Title 17, United States Code.

ProQuest Information and Learning Company
300 North Zeeb Road
P.O. Box 1346
Ann Arbor, MI 48106-1346

© 2004

Amaury Jean Henri Heresztyn

ALL RIGHTS RESERVED

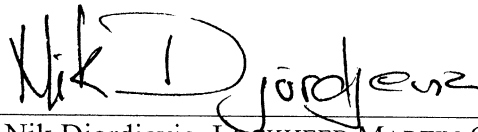
APPROVED FOR THE DEPARTMENT OF MECHANICAL
AND AEROSPACE ENGINEERING



Dr Nicole Okamoto

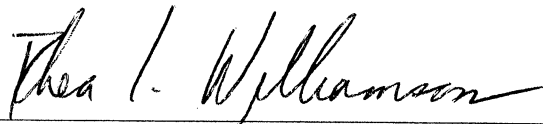


Dr Fred Barez



Dr Nik Djordjevic, LOCKHEED MARTIN CORPORATION

APPROVED FOR THE UNIVERSITY



ABSTRACT

INITIAL THERMAL DESIGN OF MICROCHANNEL HEAT SINK FOR LOW-ORBIT MICRO-SATELITES

by Amaury J.H. Heresztyn

As reduction in the size of electronics creates demand for smaller, less expensive, and faster-to-produce spacecraft, the use of high density-electronics increases the stress on the thermal subsystem.

This project intends to analyze and solve this problem. It is divided into two parts: the spacecraft thermal model and the microchannel heat sink design. First, a micro-satellite is identified by its subsystem characteristics and thermal properties. The satellite and its orbit are modeled with thermal software. To address the need for a properly designed thermal control, a computer model with high heat flux of 25 W/cm^2 is used. Secondly, the theory of single-phase liquid micro-channels Heat Sinks is applied and computer modeled to optimize a heat sink to remove $25 \text{ W}^2/\text{cm}$ over a foot print of 3.7 cm^2 . To eliminate the heat picked up by the micro-channel, a possible pumping system and radiator to be attached to the heat sink is examined.

ACKNOWLEDGMENTS

I would like to thank Dr. Okamoto, Dr. Desautel, Dr. Djordjevic, and Dr. Barez for their time, patience, and dedication and for providing me with a great education.

Also, I would like to thank the students from ME 299 for their constructive comments and Ryan Laroza from the senior satellite project class for his help on the satellite thermal modelling.

I would also like to thanks my friends and families:

Andrew and Magali for being true good friends.

Thanks to my aunties Skye and Kate for their lovely attention and for their teaching.

Thank to you “mon amour,” Kendelleski, for your help, moral support, and patience.

Thank you Matka, my mom, and Danny Booney, my dad, and Gregory my brother:

“Peu importe la distance, vous etiez toujours pres de moi.”

TABLE OF CONTENTS

Nomenclature	xi
I. Introduction	Page 1
II. Objectives	Page 2
III. Spacecraft Thermal Model	Page 3
A. Spacecraft Specifications	Page 3
B. Cubesat Subsystems Characteristics	Page 4
C. Subsystems Thermal Properties	Page 5
D. Orbital specifications	Page 5
E. Beta Angle	Page 6
F. Computer Model	Page 7
1. Results	Page 9
G. Computer Model With High Heat Flux	Page 11
III. Single Phase Liquid Microchannel Heat Sinks	Page 13
A. Main Advantages offered by water-cooled microchannel heat sink	Page 15
B. Brief overview of previous studied	Page 17
C. Theory	Page 18
1. What do we call microchannels?	Page 18
2. What do we call micro-flow?	Page 18
3. Assumptions	Page 19
4. Effects of Polarity and EDL	Page 20

IV. Microchannel Optimization for Heat Transfer	Page 22
A. Comparison of Two different models:	Page 23
1. “Micro/nano Spacecraft Thermal Control Using a MEMS-based Pumped liquid cooling system” by Birur et al. [2]	Page 23
2. “Optimization Study of Stacked Microchannel Heat Sink” by Dr. W. Wei and Dr. Y. Joshi [6]	Page 23
B. Analytical model and Benchmarking.	Page 26
1. Analytical model	Page 26
2. Benchmarking	Page 26
C. Theoretical Microchannel Heat Sink Design using Wei’s model.	Page 32
1. Influence of the Flow Rate on the Heat Source Temperature	Page 33
2. Influence of Material Conductivity on the Chip Temperature	Page 34
3. Microchannels geometric specifications	Page 36
4. Height influence:	Page 41
D. Results obtained using theoretical Microchannel Heat Sink Design	Page 42
V. Pump and Radiator Sizing	Page 42
A. Pump Sizing	Page 42
1. Pressure drop across the heat sink	Page 42
2. Different Pump Technology	Page 45
B. Radiator Sizing	Page 45
VI. Reflection and Recommendations and Conclusion	Page 47
References:	Page 50

LIST OF TABLES

Table 1: Spacecraft Configuration:	Page 4
Table 2: Subsystem Characteristics:	Page 5
Table 3: Subsystems Thermal Properties:	Page 5
Table 4: Orbital Specifications:	Page 6
Table 5: Subsystem Temperatures:	Page 12
Table 6: Convection Coefficient for three different liquids:	Page 16
Table 7: Comparison of rectangular microchannels heat exchangers for single-phase liquid water flow:	Page 17
Table 8: Reynolds' number in microchannels calculated from table 5:	Page 20
Table 9: Total Resistance Benchmarking:	Page 27
Table 10: Pressure drop benchmarking:	Page 28
Table 11: List of Material used:	Page 34
Table 12: Resistances' influence in percentage compared with mass flow rate at 10 cc/min:	Page 35
Table 13: Resistances' influence in percentage compared with mass flow rate at 100 cc/min:	Page 36
Table 14: Percentages of Resistances:	Page 41
Table 15: Results:	Page 42

LIST OF FIGURES

Figure 1: Beta Angle over one year:	Page 7
Figure 2: Temperature (K) vs. time, $\beta = -60$:	Page 9
Figure 3: Temperature (K) vs. time, $\beta = 60$:	Page 10
Figure 4: Temperature gradient of the spacecraft:	Page 12
Figure 5: Microchannels heat exchanger schematic:	Page 14
Figure 6: Pressure drop and Thermal Resistance vs. Microchannel width, Microhex:	Page 29
Figure 7: Pressure drop and Thermal Resistance vs. Microchannel width, from our model:	Page 30
Figure 8: Convection coefficient vs. Hydraulic diameter from our model, for Developing Flow:	Page 31
Figure 9: Convection coefficient vs. Hydraulic diameter from Dr. Kandilakar, for fully developed laminar conditions:	Page 31
Figure 10: Mass flow rate vs. Heat source Temperature:	Page 33
Figure 11: Conductivity Material vs. Heat Source Temperature:	Page 35
Figure 12: Channel Number & Heat Source Temperature vs. Channel Width, $w_{fin}=50 \mu\text{m}$:	Page 37
Figure 13: Channel Number & Heat Source Temperature vs. Channel Width $w_{fin}=100 \mu\text{m}$:	Page 38
Figure 14: Channel Number & Heat Source Temperature vs. Channel Width, $w_{fin}=150 \mu\text{m}$:	Page 38
Figure 15: Channel Number & Heat Source Temperature vs. Channel Width, $w_{fin}=200 \mu\text{m}$:	Page 39
Figure 16: Channel Number & Heat Source Temperature vs. Channel Width, $w_{fin}=250 \mu\text{m}$:	Page 40

Figure 17: Temperature & Pressure drop (dash line) vs. Channel Height: Page 41

Figure 18: Pressure drop in psi and heat source Temperature (dash line) vs. mass flow rate: Page 44

Nomenclature

A_c : Channel Cross Section Area, m^2

A_h : Area of heater, m^2 .

AR: Channel aspect ratio, unitless

C_p : the specific heat, in J / kg. K

d : characteristic length, m

D_h , Hydraulic Diameter, m

f : friction factor

$G(\alpha)$ = aspect ratio function

h_1 : Height Channel, m

h_2 : Height between the top of the heater and the bottom of the heat Sink, m

h : Convection coefficient, $W/m^2.K$

h_c : Height Channel, m

k : Thermal Conductivity of the material, W/mK

$K_{entrance}$: loss coefficient for the entrance in the channels.

K_{exit} : loss coefficient for the exit out of the channels

k_f : Fluid Thermal Conductivity, $W/m.K$

K_{turn} : loss coefficient due to standard 90° turn.

l_c : Channel Length, m

\dot{m} : mass flow rate, kg/sec

Nu: Nusselt number, unitless

n : number of channel, unitless

Pr: Prandl number: unitless

Q: Store heat flux, in Watts

R_{bulk} : Bulk Resistance, K/W

R_{cond} : Conduction Resistance, K/W

R_{cont} : Constriction Resistance, K/W

R_{contact} : Thermal Conductive Resistance, K/W

R_{conv} : Convection Resistance, K/W

Re, Reynolds number, unitless

R_{total} : Total Thermal Resistance, K/W

T: Temperature, in Celsius

t: time in seconds

Theater: Temperature of the heater, C

T_h : Temperature of the heater, C

T_{inlet} : temperature of the liquid at the inlet, C

V, velocity, m/s

w_c : channel width, m

w_w : Wall (fin) channel, m

y^+ : length scale for friction factor, unitless

y^* : length scale for Nusselt Number, unitless

Nomenclature: Greek Letters

α : thermal diffusivity, m^2/sec

ΔP : Pressure Drop, psi or Pa

δ_p : pressure drop, psi or Pa

η_f : fin (wall) efficiency, unitless

μ : the dynamic viscosity, $\text{N}\cdot\text{s} / \text{m}^2$

ρ : density, in kg / m^3

I. Introduction

Space programs are generally limited to very few models characterized by high cost ranging from \$50,000 to \$100,000/kg. Nowadays, considering the advancement of reduced-size electronics, there is a tendency to develop much smaller spacecraft with moderate cost and shorter fabrication time. Their payload can still include very advanced instruments such as multitask optical systems, temperature and IR sensors and cameras. Small satellites can be classified according to their weight: “nano and pico-satellite (<10kg), micro-satellites (10-100kg), mini-satellites (100-500 kg), and inter-planetary small satellite missions (>500 kg).”[1]

The development of any satellite’s subsystems is restricted by the limited size, mass, power, and bounded volume. The thermal system would be particularly challenging due to the ever-increasing power density of the electronics and the restriction of space. As we know, subsystems are inter-dependent, which creates even more constraints.

In general, a micro-satellite’s attitude control is either a free tumble or some sort of stabilization pointing at the earth or the sun. The latest pico-satellite funded by the government or academia in the last few years were mostly in free tumble, and their thermal design was based on the assumption that a truly random tumble will neutralize uneven distribution of the energy flux in and out of the external surfaces. On the other hand, for the future development of a pico-satellite with a three-axis stabilization system, i.e., no tumble, a thermal control system needs to make sure that the heat is distributed

equally between the external surfaces and the internal equipments. Every satellite component must remain in its operating range of temperature.

The function of a satellite thermal control system is to control the temperature of individual components in an ever-changing thermal environment and to ensure proper operation. Small satellites are often compared to personal computers where the system is integrated on a single chip. The power density from electronic components is expected to go as high as 25 W/cm^2 and more [2]. With a limited power, mass, and cost, the thermal control includes challenges that need to be met.

II. Objectives

The objective of this work is to develop the preliminary design of the thermal control system of a 3-axis-stabilized pico-satellite orbiting at a low-earth orbit using microchannel heat sink technology to remove high heat fluxes. This need became apparent when looking at the general design of a double pico-satellite developed by seniors at San Jose State University in 2004. Using Thermal Desktop, an extension of AutoCAD, and SINDA, the external heat transfer and the conduction path were modelled, both affecting the temperature of the spacecraft. Attention was, then, focused on integrating the model of a high power density component of 25 W/cm^2 and observing the thermal behaviour and interaction with other equipments. This showed how important thermal control of high power density components is to the rest of the Cubesat.

Indeed, when a high power density was applied to the model, the temperature for each component in the spacecraft was well beyond the operating range.

In the second part of the research, the preliminary design of a cooling system for the Cubesat using microchannel heat sink technology was undergone. To better understand microfluidic systems and micro-flows, a literature review was done over such publications as Tabeling's *Introduction à la microfluidique* [3], Gad-el-Hac's *MEMS Handbook* [4], and Nguyen and Wereley's *Fundamentals and Application of Microfluidics* [5].

In the last part of the research, a model by Dr. Wei and Dr. Joshi [6] adapted from Dr. Phillips [7] was used to optimise a microchannel heat sink in the purpose of removing $25\text{W}/\text{cm}^2$. A possible design for a pump and a radiator are also discussed. Recommendations for future work are provided in the end.

III. Spacecraft Thermal Model

A. Spacecraft Specifications

The spacecraft used for this preliminary design had the same basic configuration than the one originally conceived by the senior project student. The payload was made up of 4 different fiberglass trays. A specific subsystem was attributed to each tray: power, communication, computer, payload (camera) and attitude determination and

control (ADAC.) This configuration does not account for a high heat flux source. A summary of the basic spacecraft configuration is available in the following table:

Geometry, cm: (height*length*width)	20*10*10
Main Structure:	Aluminum Al 6061 T6
Interior	4 fiberglass trays
Weight	Less than 3 kg
Internal power (excluding the heat source)	About 5W

Table 1: Spacecraft Configuration

B. Cubesat Subsystems Characteristics

For each subsystem, the size, the wattage, the mass, and the operational temperature range were obtained. This information is very important to the thermal model. Indeed, the geometry of each subsystem and their power consumption can be entered into a computer program using finite element called Thermal Desktop. This program will be presented in detailed in part F. Once the model is finished, the temperature of each subsystem can be compared to their operational temperature range throughout a specific orbit.

It is also interesting to notice that there is an optimal temperature range between – 10 to 25 Celsius degrees. A summary of the subsystems' characteristics shows in Table 2.

system	Size (cm)	Mass (g)	Power (W)	Temperature range, C
Computer	8.6*6.4*1.0	100	0.5	.-10 < T < 70
Radio	8.9*5.3*1.8	75	1.4	.-40 < T < 70
Camera	7.6*5.1*2.1	100	0.6	.-20 < T < 60
Batteries	5.0*3.4*1.0	40	5	.-10 < T < 25
Solar Cells	2.0*2.0*0.5	0.00004	1	.-100 < T < 100
ADAC	N/A	N/A	0.525	.-40 < T < 85

Table 2: Subsystem Characteristics

ADAC stands for Attitude Determination and Control

C. Subsystems Thermal Properties

Each subsystem was attributed a value for its emissivity and its absorptivity based on the material that they are made out of. For example, the structure is made out of Aluminium 6061-T6. It will most likely be polished; therefore the value of its absorptivity and emissivity can be easily found in any thermal engineering reference book [8].

Material	Absortivity	Emissivity	Subsystem
Al 6061-T6 polished	0.08	0.031	Structure
fiberglass/Al (50-50)	0.44	0.46	electronics Components
Solar Panel	0.92	0.85	
White paint	0.23	0.8	interior

Table 3: Subsystems Thermal Properties

D. Orbital specifications

After modelling the internal heat load and heat conduction path, the orbital specifications need to be made. The spacecraft orbits at a low altitude of 600km. We choose the inclination to be 37° so that the orbit would pass right over the San Jose State University's campus location. Right ascension of ascending node, which is the celestial longitude of the point where the ascending satellite crosses the equator and the Argument

of Perigee, which is the angle between the equator and the perigee were both left at zero. We are not interested in their influence on the thermal model since the model is only used to provide a first order calculation. The model sole purpose is really just to see what the thermal behaviour of the satellite's components is when a high heat flux is applied on the spacecraft. Table 4 summarizes the principal orbital configurations.

Circular altitude:	600	km
Orbit duration:	92.5	minutes
Inclination:	37	deg
Right ascension of ascending node:	0	deg
Argument of Perigee:	0	deg
Eclipse duration:	37	min/orbit

Table 4: Orbital Specifications

E. Beta Angle

One of the most important parameters in determining the thermal control of a spacecraft at a low orbit is the beta angle. It is defined as the minimum angle between the orbit plane and the solar vector and can vary from -90 to $+90$ deg [9]. It is a function of the declination of the sun, orbit inclination, right ascension of the ascending node, and right ascension of the sun. The angle varies all the time through the year. In other words, the beta angle will determine how much heat load the spacecraft is receiving from the direct solar input and from the Earth reflection of the sun or so called Albedo. Using the software called STK (Satellite Tool Kit), we were able to obtain the different values of the beta angle over the cycle of year of 2003.

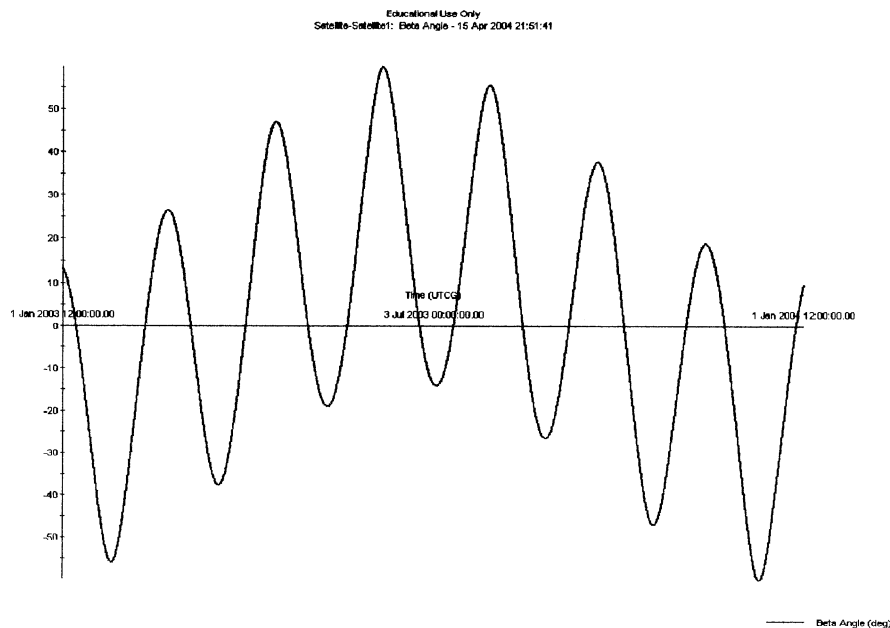


Figure 1: Beta Angle over one year

F. Computer Model

The software used to model the spacecraft is an extension of AutoCAD called Thermal Desktop combined with the thermal model compiler named SINDA. The compiler is a thermal analysis code that is made of preprocessor and execution library and uses the Taylor Series Approximation to solve for the thermal math model. This combination offers the opportunity to model the spacecraft throughout a desired orbit. Thus, the influence of the external heat loads, varying because of the beta angle, can therefore easily be accounted for. Also, different operating modes of the satellite can be modeled. For example, one can turn the battery on and off and see its thermal influence on the rest of the spacecraft.

In our model, each subsystem and each part of the spacecraft structure were only reproduced in two dimensions (2D). In other words, the thickness was not modeled since it is not believed to be crucial to represent heat transfer between components. At the “First Developer Cubesat Conference” in San Luis Obispo (April 2004), many universities presented a similar method for the thermal model.

Concerning the grid, the cells’ sides were set to 5mm in the x and y directions or also called length and width of every different panel and subsystems. Thus, 800 cells were assigned for the long external panel (10cm*20cm). The shorter exterior panels (10cm*10cm) and the subsystem trays ended up having 400 nodes each. The same grid size was used for the subsystem’s models: 5mm for the length and width of each subsystem. The grid size is thought to be adequate to represent the heat transfer throughout the satellite. This computer model is only being made to approximate how hot the spacecraft will get, showing the need for innovative cooling techniques. Therefore, a more precise and detailed grid generation study is not needed.

The heat conduction path inside the satellite is maximized as each panel is entirely connected to its neighbors. We understand that the number of nodes might not be sufficient to obtain a thorough model but it is sufficient for us to understand how heat propagates in the spacecraft. Eventually, it will also be helpful when locating pumps and radiators.

Once the drawing and modeling is finished, the calculation can start. A source code representing the spacecraft model is sent to the compiler named SINDA. The results are then processed and made available through different output: a graph of the temperature

versus time for any selected subsystem and/or a color representation of the spacecraft nodes. In the last case, each color corresponds to a certain range of temperature.

1. Results

The two extreme beta angles were modeled. Figure 3 shows the temperature of the spacecraft with respect to the time at a beta angle of -60 degrees. In the very beginning, the initial conditions were set as if the temperature was about 290 K, the standard atmospheric temperature as if the model were being taken out of the standard atmosphere and put right out into space. After a series of iterations, SINDA provides a solution with a constant pattern for each completed orbit. Indeed, at $t = 10,000$ seconds, the temperature remain around 240 K. The 5000 seconds orbit increments is then easily spotted on the graph.

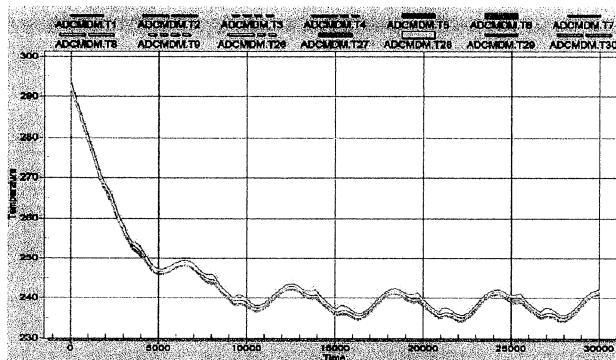


Figure 2: Temperature (K) vs. time, beta =-60

Figure 3 shows the temperature of the spacecraft with respect to time with a beta angle of 60 degrees. After iterations, the results show the temperature of each subsystem, throughout three full orbits, getting hotter in the sun and cooling off during the eclipse.

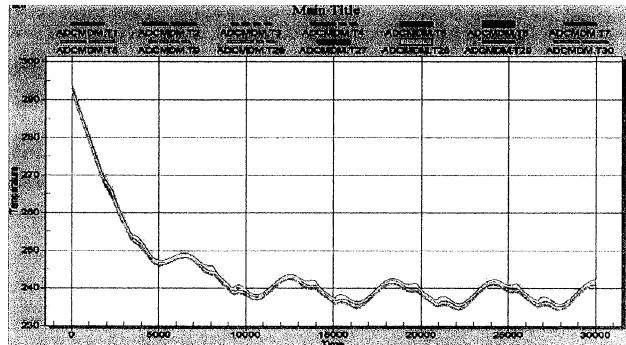


Figure 3: Temperature (K) vs. time, $\beta = 60$

The model that we defined and the results that we obtained are well in accordance with the one found by previous school programs. Those results were presented at the "First Developer Cubesat Conference" held in San Luis Obispo in April 2004 [9]. The spacecraft ends up being very cold several degrees below zero Celsius. Most of the time to prevent any freezing of any components such as the battery, a heater is attached.

For the satellites that have been put in orbit, the temperature sensors have registered higher temperature than the one predicted by their computer model, which might show that the model is, in fact, conservative.

G. Computer Model with High Heat Flux

Keeping the same model that we have just been discussing, a component with a high heat flux source was implanted. This component could be anything: from a reduced-size computer chip to a small nuclear power system. In the purpose of this project, the source with a high flux is what is the most important. Based on Dr. Birur's expectations of future needs [2], the heat flux was modeled to be of the order of $25\text{W}/\text{cm}^2$ over an area 3.7cm^2 . Indeed, Dr. Birur has been working on integrating a similar cooling design to a micro-satellite and has been using the previously mentioned parameters in his research. In order to compare our result to Dr. Birur's and to improve them, the same parameters concerning the heat flux will be used. The source was simply attached to the model using the surface to node command.

Figures 4 and Table 5 show the result of the model. Most of the spacecraft is well above 350K. Having the high heat flux source implanted on the second tray starting from the bottom, it is interesting to notice that the source area has a temperature above 450K. The tray supporting the source has a temperature above 380 K and we can see the heat propagating to the bottom tray, above 350K. The upper part of the spacecraft is below 350K. One can explain this behavior when taking into account the orientation of the satellite in this case. Indeed, the bottom part of the satellite is facing the earth and is acting as a shield to the upper part of the satellite. Then the upper part is not shined upon by the earth's reflection or the sun.

The heat flux of $25\text{W}/\text{cm}^2$ is the reason why the temperatures are so high. That is why we need to a better heat removal mechanism to keep the electronic components in an acceptable range of 60 to 80 Celsius degrees depending on the application.

	Max (K)	Min (K)
ADAC	348	335
Trays	380	331
Camera	361	360
Computer	372	368
Upper Part	331	330
Heat Source	1858	1800
Battery	335.17	330

Table 5: Subsystems temperatures

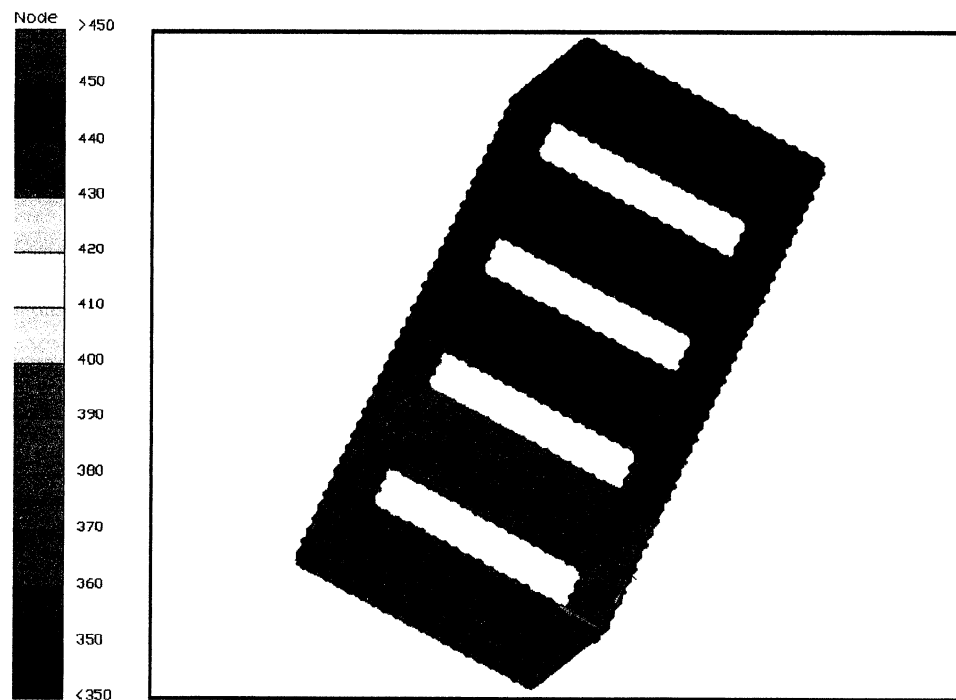


Figure 4: Temperature gradient of the spacecraft.

These models are not entirely complete. It would be interesting to have range of temperature for the different operating modes: battery charging, discharging, camera on

and off, etc. A better model could be achieved improving, for example, the assumptions on the thermal properties of most subsystem. On the other hand, the primary purpose with these models has been reached, which was to approximate how hot the temperature of spacecraft becomes when a high heat flux is applied and how important it is to design the proper thermal control. The future use of these models will be important when developing the thermal control subsystem and its integration into the satellite.

III. Single Phase Liquid Microchannel Heat Sinks

For two decades, many researchers and companies in the industry have focused their efforts on a new heat management technology called a microchannel heat sink. A pumped liquid or gas is sent through the channels of a heat sink. A high heat flux source is connected to the bottom of the heat sink. Heat travels from the hot source to the cooler liquid in the channel. And the water inside the channel is getting warmer and can essentially travel the heat anywhere. Please refer to Figure 5 taken out of Dr. Birur's publication:

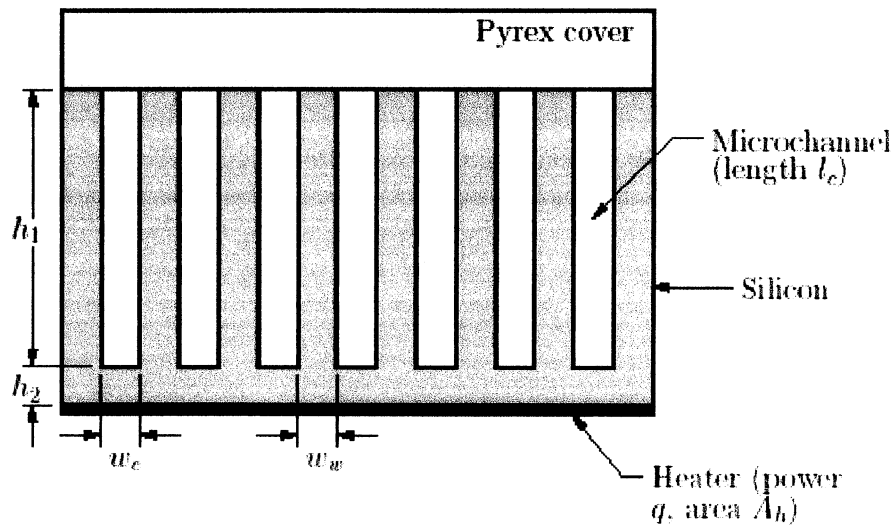


Figure 5: Microchannels heat exchanger schematic. [2]

There are many different ways to approach this design. One can use single-phase liquid or gas. Also, boiling and condensation can be used in the channel in order to increase the heat removal. The shape of the channels, their dimensions, aspect ratio, and the mass flow rate, all play an important role in optimizing the design of a microchannel heat sink. Because of the challenges associated with boiling in microchannels, especially in a zero-gravity environment, we decided to only look at the design of single-phase liquid microchannel heat sink.

First, let us look back at the reasons why single-phase liquid microchannel are a good solution to remove hot spots. We will briefly report what other studies already published. Then, we will present the theory of microchannels and define micro-flows. Having our focus on removing large heat flux from small hot spots, we will look into the design of an efficient microchannel heat sink using published models.

A. Main Advantages offered by water-cooled microchannel heat sink

This thermal management method shows many advantages. Liquids such as water have a much better thermal conductivity than the air blown over a heat sink. Indeed, in a liquid, the molecules are closer to one another enhancing heat transfer. Liquids offer a higher specific heat. Also, with microchannels heat exchanger, there is no contact between the fluid and the hot component, which prevent components short circuit by the fluid.

As we all know, the stored heat flux Q is presented as

$$Q = \rho \times C_p \times \frac{\partial T}{\partial t}$$

Where ρ is the density, C_p is the specific heat, $\frac{\partial T}{\partial t}$ is the temperature change with respect to time.

Therefore, as Tabeing [3] puts it, the time of heat transfer associated to an object of dimension L can be written as

$$\tau = \rho \times C_p \times \frac{L^2}{K}$$

$$\tau = \frac{L^2}{\alpha}$$

where α stands for the thermal diffusivity (m^2/sec). [3]

The cooling time would be reduced if a high diffusivity and small sizes are used at the same time.

Microchannels have another main advantage, as Gad-el-Hak presents it, [4].

Despite the fact that they have a small volume, the channels offer very important surface area, which helps to dissipate the heat to the cooling fluid. More of the fluid is in contact with the hot spot.

Finally, when the flow is laminar and thermally developed in the channel, the Nusselt number remains constant and so does the convection coefficient h :

$$Nu = h \times \frac{d}{k_f} = \text{constant}$$

So the convection coefficient h is proportional to the inverse of the characteristic length d . When d decreases, the convection coefficient h increases. For example, for a characteristic length d of 0.1 mm and a Nusselt number Nu of 4.36 (for a circular tube and uniform surface heat flux), we can get the following value for the convection coefficient h :

	k , W/m.k	h , W/m ² .K
Ethylene Glycol	0.242	10550
Freon	0.073	3180
Water	0.6	26160

Table 6: Convection coefficient for three different liquids

B. Brief overview of previous studies

The idea of fabricating microchannel heat sinks is not new. Tuckerman and Pease first introduced it in 1981. They were able to dissipate a heat flux as high as 790 W/cm² [9]. Following this discovery, many researchers have been trying to understand this phenomenon better. Birur published a comparison of research on rectangular microchannel heat exchangers for single-phase liquid water flow, here shown in table 5. [2]

Investigators	Substrate	$A_h(A_c)$ cm ²	l_c cm	h_1 μm	$w_c(w_w)$ μm	q W	Q cc/s	R_{total} °C/W	ΔP kPa
Harms <i>et al.</i>	Silicon	6.25 (6.25)	2.5	1030	251 (119)	415	46.3	0.041	30.5
Tuckerman	Silicon	1.0 (2.8)	1.40	302	50 (50)	790	8.6	0.090	214
Cuta <i>et al.</i>	Copper	4.06 (4.06)	2.05	1000	270 (270)	402.5	3.49	0.168	20.7
Kishimoto and Ohsaki	Alumina	16.0 (62)	8.6	400	800 (1740)	380	13.3	0.132	-

Table 7: Comparison of rectangular microchannels heat exchangers for single-phase liquid water flow

Each entry can be referred to the following drawing published by Birur [2] see figure 5.

One can appreciate the small size of those heat sinks. They are not higher than a couple hundred micrometers (μm) and their length averages around 2 centimeters (2 cm). Most of them have a silicon substrate, which is the component in which the channels are made.

C. Theory

1. What do we call microchannels?

According to Gad-el-Hak, microchannels dimensions ranges from $1\mu\text{m}$ to 1mm . He also explains than anything “above $1\mu\text{m}$ the flow exhibits behavior that is the same as most macroscopic flows. Below $1\mu\text{m}$, the flow is considered nanoscopic.” Most microchannel heat sink are designed within a range of 30 to $300\mu\text{m}$. [4]

As described by Birur [2] and Gad-el-Hak [4], the method of fabrication comes from the electronics industry. Looking back at table 5, the channels are embedded in the substrate, which is most of the time made out of silicon, copper and Alumina, or glass, polymers and metals [4]. Different processes are used such as surface machining, bulk machining, molding, etc.

2. What do we call micro-flow?

Most of the books in the academia model fluids as a continuum. Instead of looking at each and every molecule, they just look at the average effect on a number of molecules. Is this model valid for microchannels flow?

As Tabeling [3] and Gad-el-Hak [4] reminds us, this model only works if the size of the particles is small compared with the size of the mean free path. Many molecules make up fluid particles, which are still of a size of a couple nanometers. Since the

microchannels are of the order of the micrometers, the continuum model can be used with no problem when applied to liquids.

3. Assumptions

As stated earlier, microchannels offer a large surface-to-volume ratio, which enhance the surface forces. Therefore, gravity can be neglected compared to the surface forces. Indeed, you have very little liquid, so its weight is not so important. But, since the liquid is in contact with much surface, it can be easily seen how surface forces are much more important [4]

The liquid flow can be considered laminar. Let's take a critical Reynolds number of 2300 for rectangular channels. Reynolds number is defined as

$$\text{Re} = \rho \times V \times \frac{D_h}{\mu}$$

where ρ is the density of the liquid, V the velocity, μ the dynamic viscosity, and D_h the hydraulic diameter defined as

$$D_h = 4 \times \frac{A_c}{P}$$

Where A_c and P are the flow cross-sectional area and the wetted perimeter, respectively.

Based on the cases reviewed by Birur in table 5, we get the following Reynolds numbers with a fluid temperature of 20C

Investigators	Dh, m	channels #	V in 1 channels, m/s	Re #
Harms et al.	0.000404	68	2.65	70
Tuckerman	8.58E-05	71	7.97	45
Mahalingam	0.000358	96	1.92	45
Kishimoto	0.000533	7	5.67	199
Sasaki*	0.000494	16	N/A	N/A
Riddle et al.	8.80E-05	64	17.2	100
Cuta et al.	0.000425	37	0.35	10

Table 8: Reynolds' number in microchannels calculated from table 5

*Certain values are not available so we cannot obtain Re.

The Reynolds number, as described below, is very low, which supports the case for high shear forces. Indeed the Reynolds number is the ratio of inertia forces over shear forces. For a small Reynolds number, high shear forces are involved.

Therefore we can see that our assumption of laminar flow is a good one. Also, The flow is assumed to be steady and incompressible. The heat flux, coming from the high density heat source, is considered to be uniform and constant. The thickness of the channel is supposed to be uniform. The cover plate is adiabatic. Radiation heat transfer are negligible. There are no gravity force but only contact forces such as viscous forces.

4. Effects of Polarity and EDL

Polar mechanics can have an influencing effect on a fluid inside a microchannel. As opposed to the macro level, molecules in microchannel can really be influenced by polar mechanics. As describe by Gad-el-Hak [2], "In micro-polar fluid theory, the laws

of classical continuum mechanics are augmented with additional equations that account for conservation of micro-inertia moments.”

Moreover, the electric double layer can also influence the flow. Gad-el-Hak wrote that “When a liquid containing a small amount of ions is forced through a microchannel under hydrostatic pressure, the solid-surface charge will attract the counter-ions in the liquid to establish an electric field. The arrangement of the electrostatic charges on the solid surface and the balancing charges in the liquid is called the electric double layer (EDL).” Therefore, the EDL and the micro-polar effects modify the flow pattern and the velocity distribution defined by the classical model. Then, heat transfer can be modified as well.

However, Gad-el-Hak report that these phenomenon’s effect have not yet been fully understood and neither approved [2]. Some researchers have proven these effects to modify heat transfer whereas others contradict this theory. In one research, the micro-polar effects were measured and it was realized that the classical model was far off from reality. But Gad-el-Hak underlines that “the difference between the results of the two theories is smaller than the difference between the experimental data and the predictions of either theory.” The cross section of the channels in this case were $600\ \mu\text{m} * 30\ \mu\text{m}$. In the model we expected to create, the channel height would be around $600\ \mu\text{m}$ but the channel width might be ten times bigger.

In another case, where the channel cross section was $20\ \mu\text{m} * 2\ \mu\text{m}$, measurements of the water flow were made and the classical model was found to be verified by the experiments measurement. As put by Gad-el-Hak, “However, more research work is

required to verify these observations, as these discrepancies may have to do more with experimental errors rather than true size effects.” [2]

Some researchers have specialized in the interaction of the EDL and the micro-polar effect on the heat transfer, [10]-[11]. But we are not going to discuss these any further. From now on, the assumptions will be made that these phenomena do not interact with flow. Indeed more research needs to show that classical model needs to be modified to include the polar and EDL effect. Moreover, most research publications concerning heat transfer in microchannel heat sink all use the classical model.

IV. Microchannel Optimization for Heat Transfer

To understand how heat transfer works, we have concentrated on two different papers: “Micro/nano Spacecraft Thermal Control Using a MEMS-based Pumped liquid cooling system,” written by Dr. Birur [2], “Optimization Study of Stacked Microchannel Heat Sink” by Dr. Wei and Dr. Joshi [6].

The Birur research paper offers a good summary of previous studies and also presents results of an experiment. Dr. Birur was efficiently removed $5\text{W}/\text{cm}^2$ of heat from a 3.7 cm^2 foot print using water as the working fluid. On the other hand, Wei and Joshi bring us an analytical model of a stacked microchannel heat sink that we are going to use as the basis for our single microchannel heat sink. Then, we will try to optimize the analytical heat sink for the purpose of removing $25\text{W}/\text{cm}^2$ from a 3.7 cm^2 foot print.

A. Comparison of Two different models:

1. “Micro/nano Spacecraft Thermal Control Using a MEMS-based Pumped liquid cooling system” by Birur et al. [2]

Birur uses a numerical model, based on MICROHEX, a FORTRAN code created by Phillips [7]. This model uses the thermal resistance network technique. The assumptions that we have listed earlier are valid. There are also a few more: uniform fin-base temperature, identical fin-base and channel-base temperature and a uniform coolant temperature and heat transfer coefficient at a given axial distance.

In this paper, Birur shows the results of an experiment where the pressure drop, the chip average temperature and the exit tubing temperature are reported for steady state for a flow rate of 9cc/min and 20 Watts of power applied. In the end, the chip temperature was about 43°C with heat flux at about 5.4 W/cm² and a pressure drop of 20psi and liquid temperature at exit of 33°C.

Birur’s experimental results will be used as a starting point of the design. We will try to attain those results and to improve the design so that we can reach a cooling capacity of 25 W/cm².

2. “Optimization Study of Stacked Microchannel Heat Sink” by Dr. W. Wei and Dr. Y. Joshi [6]

Wei and Joshi's research paper discusses optimizing the removal of heat fluxes using microchannel heat sinks stacked on top of each other. However, this model will only be used for one heat sink. We are not interested in the stacking option as space and weight are driving factor of the design.

Just like in the previous case, their model was based on the one created by Phillips [7]. Thus, the same assumptions are made. Even though, Wei and Joshi are using the thermal resistance network technique, their resistances are not computed the same way. They have introduced a constriction resistance, which is caused by the area change between the base and the fin and a modified convection resistance. The conduction and bulk resistances are defined the same way.

The thermal performances depend on the total thermal resistance: R_{total}

$$R_{total} = \frac{(T_{heater} - T_{inlet})}{(\text{power applied } Q)}$$

$$R_{total} = R_{cond} + R_{cont} + R_{conv} + R_{bulk}$$

R_{cond}

R_{cond} = conductive resistance between the heated surface and the channels

$$R_{cond} = \frac{h_2}{(k \times A_h)}$$

R_{cond} = length from heater to microchannels / ($k_{material}$ * foot print area)

R_{cont}

R_{cont} = Constriction resistance taking the area change into account

$$R_{\text{cont}} = (w_{\text{fin}} + w_c) \times \frac{\text{Ln} \left(\sin\left(\frac{\pi}{2} \times \left(1 + \frac{w_c}{w_{\text{fin}}}\right) - 1\right) - 1 \right)}{(k * A_h)}$$

The constriction resistance included here is different from the one published in Wei and Joshi's Paper. Indeed, it seems as if the addition of the thickness of the wall to the width of the channel was missing from the print: $(w_{\text{fin}} + w_c)$. On the other hand, this term is necessary in order to conserve the same units throughout all thermal resistances. The corrected constriction resistance R_{cont} was obtained from Incropera [12]

R_{conv}

R_{conv} = convection resistance between the microchannels and the fluid

$$R_{\text{conv}} = \frac{1}{(h \times n \times \text{Length} \times \text{width} + 2 \times h_f \times \eta_f \times \text{Length} * \text{Height})}$$

R_{bulk}

R_{bulk} = resistance from the bulk temperature rise of the working fluid from the inlet.

$$R_{\text{heat}} = \frac{1}{\rho \times C_p \times V \times n \times h_c \times w_c}$$

Here n is the number of channel, η_f is the fin efficiency and h is the convection coefficient, which is obtained from the Nusselt number using a "Churchill-Usagi Asymptotic" model. In this case the Nusselt number is expressed as a function of the channel aspect ratio. The characteristic length is taken to be the square root of the channel cross-sectional area. Computing the Nusselt number following the same fluid properties and the same channel geometry than in Birur's case, we found a value of 4.03.

B. Analytical model and Benchmarking.

1. Analytical model

The analytical model used to represent the heat transfer in the microchannel heat sink is similar to the one use by Dr. Wei. The conduction, the convection and the bulk resistance are similar. On the other hand, a contact resistance between the heater (chip) and the heat sink has been added. Its value is kept constant at $R_{\text{contact}}=0.00157\text{W/K}$. This value is based on a thermal grease called Artic Silver IV [13]. Also the thermal resistances network is related to the total power Q emitted by the heater by the following equation:

$$R_{\text{total}} = R_{\text{cond}} + R_{\text{cont}} + R_{\text{conv}} + R_{\text{bulk}} + R_{\text{contact}}$$

$$R_{\text{total}} = \frac{(T_{\text{heater}} - T_{\text{inlet}})}{Q}$$

2. Benchmarking

The model that has just been described is made up of several important heat transfer entities: the total resistance R_{total} , the convection coefficient h , the Nusselt number Nu . Since it is needed to specify the pump, pressure drop is also a key point.

To verify the validity of our model, it has been run against published data from Dr. Birur publication, Dr. Rahman's experimental measurement [14] and Dr. Kandlikar's research [15]. Dr. Rahman's published results from experimental measurements of heat transfer coefficient in different configuration of microchannel heat sink where water was the working fluid. Dr. Kandlikar presents the evolution of microchannels flow and offers a very elegant summary of the work done on this new technology.

Total Resistance R_{total}

Birur published a table summarizing results from previous experiment run by different researchers: Tuckerman, Harms et al, Kishimoto and Ohsaki, Cuta et al. and Riddle. The table below shows the result from Birur publication. A column explains if the result were calculated or obtained from experiments. The third column reports the result obtained with our new model with the same parameters used for data reported by Dr. Birur. The last column represents the difference between the results reported by Dr. Birur with the results obtained with our model. The resistance unit is in K/W.

	R_total published	Measured/estimated	R_total We	Difference, %
Tuckerman	0.09	Measured	0.08485	-5.72
Harms et al.	0.041	Measured	0.06557	59.93
Kishimoto & Ohsaki	0.132	estimated	0.1007	-23.71
Cuta et al.	0.168	estimated	0.1605	-4.46
Riddle	0.06806	estimated	0.06909	1.51

Table 9: Total Resistance Benchmarking

As one can see the results are within 6% for all cases but for Harms et al. and Kishimoto and Ohsaki, where the difference is about 60% and 24% respectively. One can try to explain this large discrepancy between Harms et al. and the current model. Their resistance was measured and in the micro world measurements can become very difficult to perform accurately.

Pressure drop across the heat sink

The same results published by Birur were used to compared the pressure drop. The table below shows: the result from Birur publication, the result obtained using our model and difference between the results as a percentage. All results from the experiments were measured. Kishimoto and Ohsaki's results were not available.

	Pressure Published (kPa)	Pressure calculated (kPa)	difference, %
Tuckerman	214	224	4.67
Harms et al.	30.5	33.144	8.67
Kishimoto & Ohsaki	?	19	N/A
Cuta et al.	20.7	16.68	-19.42
Riddle	500	507	1.40

Table 10: Pressure drop benchmarking

As one can see, in all cases, our model verifies the published results within a satisfying range.

Pressure and Total Resistance vs. Microchannel width

The following graph was published in Dr. Birur's paper and was produced with a model named Microhex developed by Phillips [7]. It shows the pressure drop and the total resistance measured for a heat sink with the following specification: a channel height of 400 μm , the channel width is equal to the fin width and the length and the surface area are fixed at 2 cm and 3.5 cm^2 respectively. Our model was run using these same parameters. The results are shown in Figure 7. The pressure pattern is very

similar. On the other hand, at $100\mu\text{m}$, the pressure drop differs by as much as 50%. However, experimental measurements may be needed as viscous forces are expected to create more of a pressure drop. One may notice that the resistance obtained with the model is a bit higher by 20% for a microchannel width of $400\mu\text{m}$. This means that the current model can be considered conservative.

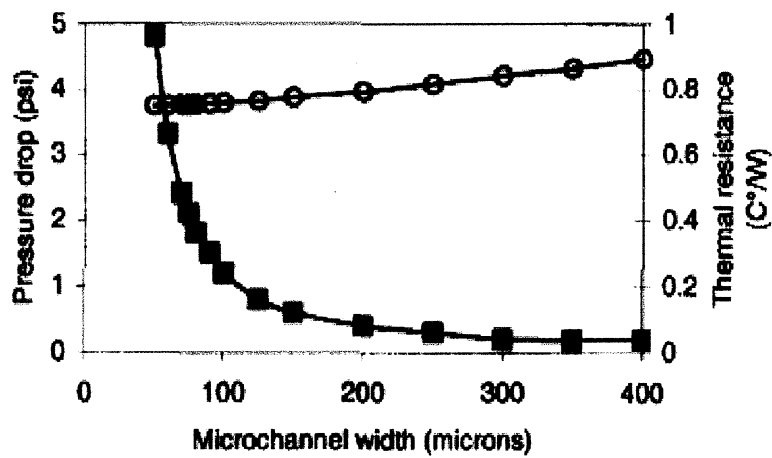


Figure 6: Pressure drop (square) and Thermal Resistance (circle) vs. Microchannel width, Microhex

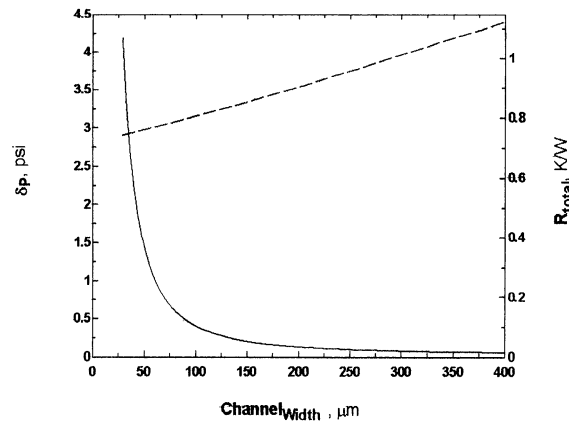


Figure 7: Pressure drop Continuous and Thermal Resistance (dash) vs. Microchannel width, from our model

Convection coefficient h vs. hydraulic diameter D_h

Convection coefficients are analytically obtained from the Nusselt number. In the new model that has been presented, the Nusselt number is adopted from a Churchill-Usagi asymptotic type of model [6] where,

$$G(\alpha) = \frac{1}{1.0869571^{1-\alpha}(\sqrt{\alpha} - \alpha^{\frac{3}{2}}) + \alpha}$$

$$y^* = \frac{y}{\text{Re}_{\sqrt{A_c}} \times \text{Pr} \times \sqrt{A_c}}$$

$$\text{Nu} = \left[\left(0.501 \times \left(\frac{8 \times \sqrt{\pi} \times G(\alpha)}{y^*} \right)^{1/3} \right)^5 + \left(3.66 \times \frac{G(\alpha)}{\alpha^{0.1}} \right)^5 \right]^{0.2}$$

Dr. Kandlikar shows variation of heat transfer for a square channel under laminar flow and constant heat flux. The first figure has been obtained with the model. The second comes from Dr. Kandlikar's research on Thermohydraulic performance for microchannels.

One may notice that for both graph, the convection coefficient varies from above $h = 10,000 \text{ W/m}^2 \text{ K}$ to about $h = 1000 \text{ W/m}^2 \text{ K}$. Thus, a small hydraulic diameter will ensure a high heat transfer. On the other hand, small channels induce higher pressure drop. One may notice that the difference in the curves' behaviors. In the first figure, the flow is still developing whereas, in the second figure, the flow is fully developed in laminar conditions. When the flow is developing, the heat transfer is enhanced.

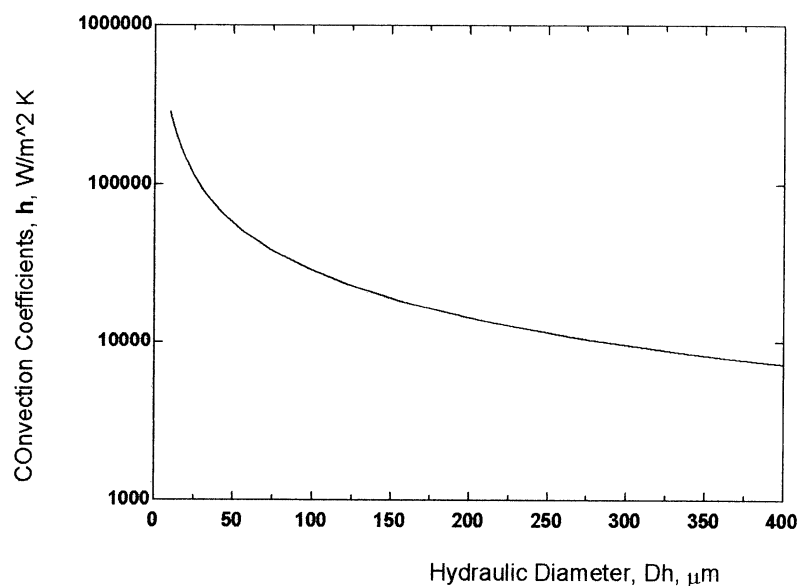


Figure 8: Convection coefficient vs. Hydraulic diameter from our model, for Developing Flow.

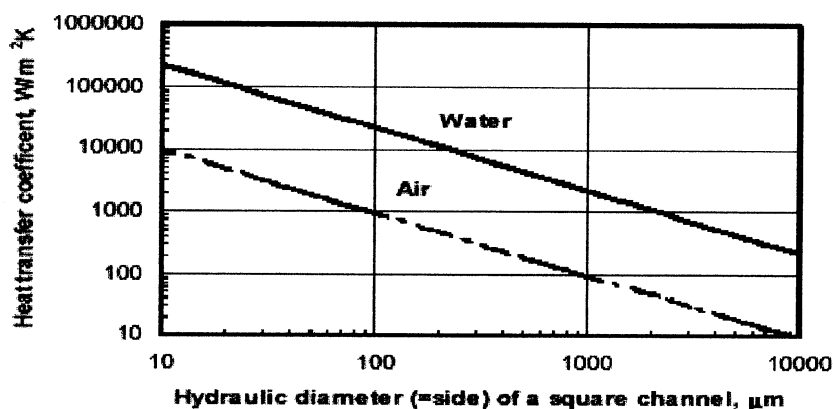


Figure 9: Convection coefficient vs. Hydraulic diameter from Dr. Kandilakar, for fully developed laminar conditions [15]

Nusselt Number:

In this part of the benchmarking review, the Nusselt number obtained with the new model are compared to one measured by Dr. Rahman during his experiments. Dr. Rahman presents Nusselt number for micro heat sink obtained through experiments [14]. Water mass flow rate was measured by collecting water mass over a time interval. Different type of thermocouple recorded temperatures, with an accuracy within 0.1°C , at several locations along the wafer wall in which the microchannels were made. Constant heat flux was provided through electrical resistances. Their calculated values for the Nusselt numbers vary from 10 to above 30 for Reynolds number varying from 1000 to 3000. Running the same parameters, with the modified new model, we found our Nusselt number to vary between 5 to 10.

One can safely say that the model is conservative. The reason why Rahman's Nusselt numbers are higher may come from the important surface roughness he measured in his microchannels. The depths of every microchannel were measured and it turns out that the surface roughness can be as high as a dozen microns. Indeed, the roughness breaks the laminar boundary layer and turns the flow turbulent, increasing greatly the heat transfer coefficient, therefore increasing the Nusselt number.

C. Theoretical Microchannel Heat Sink Design using Wei's model.

In this part of the research, a microchannel heat sink is optimized using the model derived earlier in the purpose of removing 25 W/cm^2 . The temperature of the heat source

should not be higher than 70 to 100C, which is the value at which computer chips are rated to operate. The water entering the heat sink is kept at 20C.

1. Influence of the Flow Rate on the Heat Source Temperature

Figure 10 shows source temperature versus mass flow rate. In this case, the material used is Copper with a Thermal Conductivity of $k = 401 \text{ W/mK}$. The microchannel heat sink specifications are the following: number of channel = 50, Channel width = $200\mu\text{m}$, fin width = $150\mu\text{m}$, Foot-print = 3.5cm^2 , length = 2 cm, width = 1.75cm , channel height = $400\mu\text{m}$.

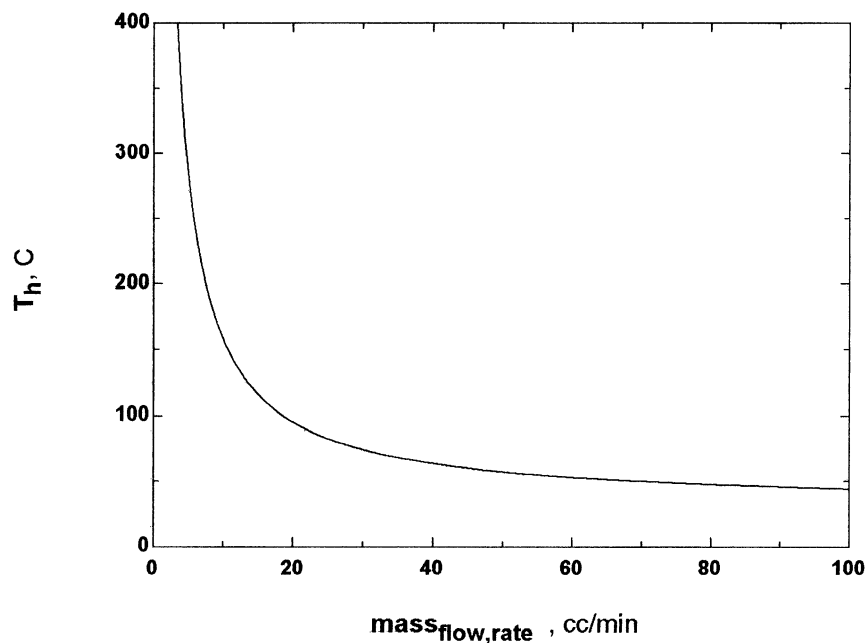


Figure 10: Mass flow rate vs. Heat source Temperature.

It is interesting to notice that after a mass flow rate of 6 cc/min, the heat source temperature reaches 100 C. This is important information since a lower flow rate allows for a smaller pressure drop and also a smaller pump, which will save weight in the thermal subsystem of the satellite.

2. Influence of Material Conductivity on the Chip Temperature

Different materials are introduced in the model to see how the temperature of the heater changes as shown in Table 9. The microchannel heat sink keeps the same specification through this model except that the mass flow rate is set to 10cc/min .

	k, W/mK	T _{heater} , C
Pure Aluminum	237	159.4
Gold	317	158.5
Pure Copper	401	155.8
Silver	429	157.8
Graphite pyrolitick, // to layer	1950	155.7
Carbon Type Ila	2300	155.6

Table 11: List of Material used.

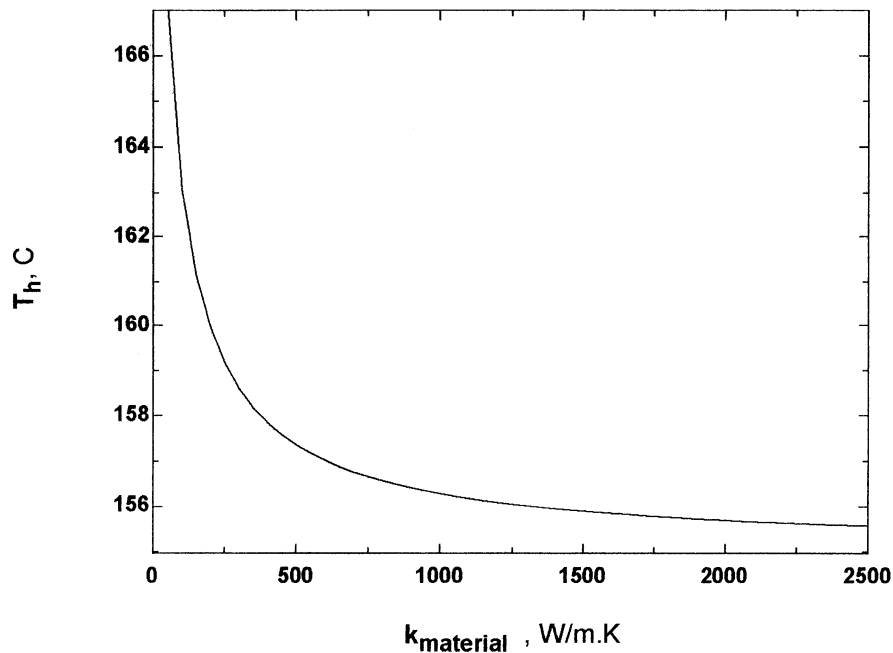


Figure 11: Conductivity Material vs. Heat Source Temperature.

One can easily see that the thermal conduction has only a small effect on the temperature of the heat source. The temperature changes only a few degrees while the conductivity of the heat sink material changes from 50 to 2500 W/mK.

Choosing copper as the heat sink material due to its high conductivity and its low cost and keeping a mass flow rate constant at 10cc/min with the specification mentioned earlier, we get the following table:

	R_contact	R_bulk	R_cond	R_cont	R_conv	R_total
Resistance, K/W	0.00157	1.437	0.000713	0.000375	0.1373	1.576958
Percentage of total, %	0.099559	91.12482	0.045182	0.023799	8.706638	100

Table 12: Resistances' influence in percentage compared with mass flow rate at 10 cc/min

With a mass flow rate increased to 100 cc/min, the influence of the resistance become:

	R_contact	R_bulk	R_cond	R_cont	R_conv	R_total
Resistance, K/W	0.00157	0.1437	0.000713	0.000375	0.1351	0.281458
Percentage of total, %	0.55781	51.05561	0.253146	0.133341	48.00009	100

Table 13: Resistances' influence in percentage compared with mass flow rate at 100 cc/min

One may notice the importance of the mass flow rate has on the thermal bulk resistance. Also, the convection resistance has now become important. The convection resistance is function of the microchannel specifications, the mass flow rate, and the fluid properties. From now on, the aim will be to lower the convection resistance.

3. Microchannels geometric specifications

The mass flow rate is regulated by any given pump, which makes it easy to change at any moment. On the other hand, the convection resistance is depends on the geometry or parameters attributed to the microchannel and heat sinks width, length and height.

The area of the foot print was kept constant: $A = 3.5 \text{ cm}^2$ and the length remained the same: $L_c = 2 \text{ cm}$. Therefore the width of the heat sink was limited to 1.75 cm. Also the flow rate was set at 70cc/min as an average between the previous assigned mass flow rate. The width of the channel was modified and the temperature of the heat source will be calculated along with the number of channel for the following 5 cases:

$$w_{fin} = 50 \mu\text{m}, w_{fin} = 100 \mu\text{m}, w_{fin} = 150 \mu\text{m}, w_{fin} = 200 \mu\text{m}, w_{fin} = 250 \mu\text{m}.$$

In the following graphs, the continuous line (—) corresponds to the number of channels and the dashed line (----) represents the heat source temperature.

Case 1: Fin width, $w_{fin} = 50 \mu\text{m}$

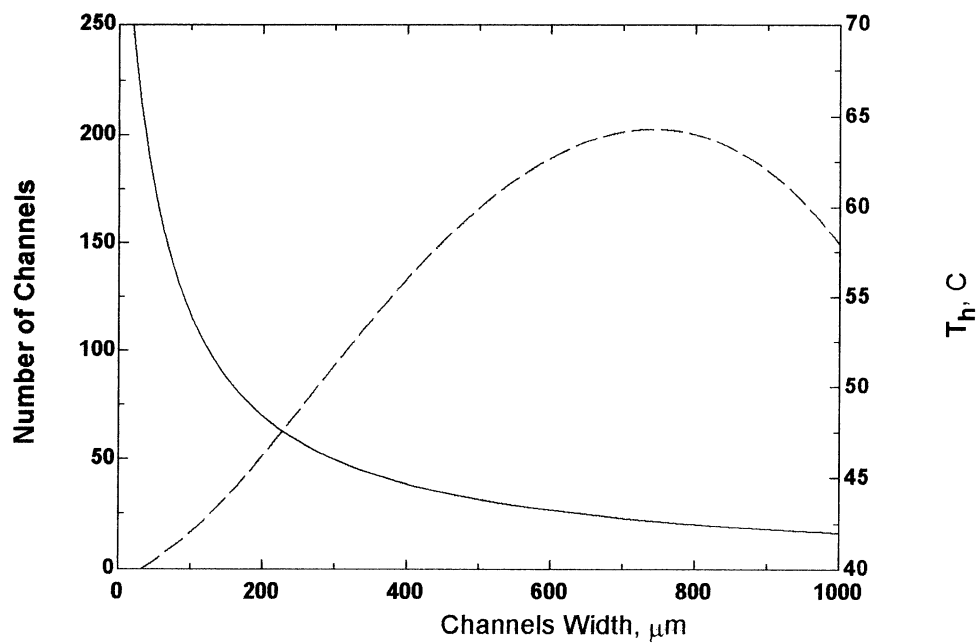


Figure 12: Channel Number & Heat Source Temperature vs. Channel Width: $w_{fin}=50 \mu\text{m}$

Case 2: Fin width, $w_{fin} = 100 \mu\text{m}$

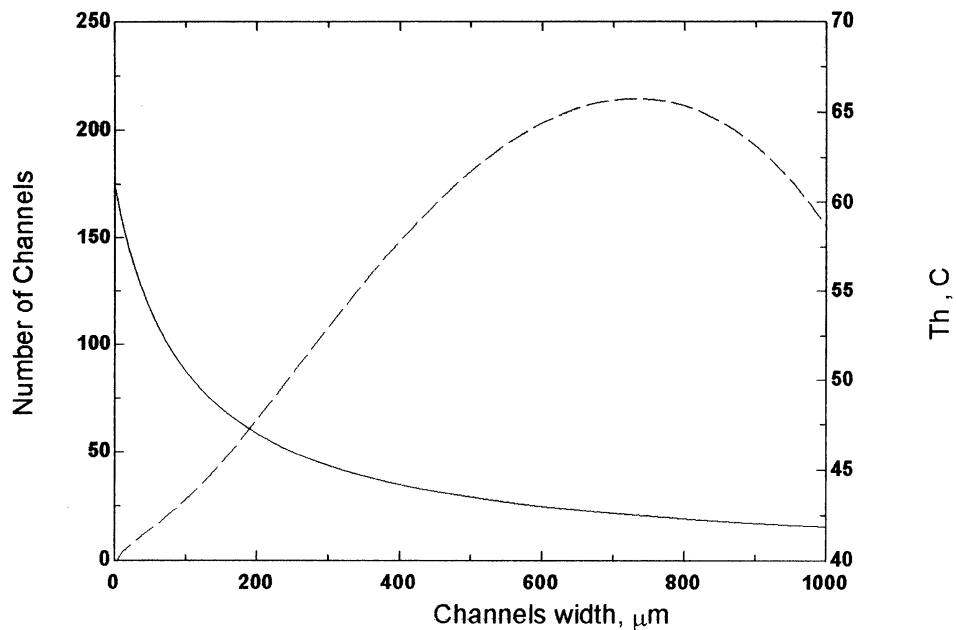


Figure 13: Channel Number & Heat Source Temperature vs. Channel Width $w_{fin}=100 \mu\text{m}$

Case 3: Fin width, $w_{fin} = 150 \mu\text{m}$

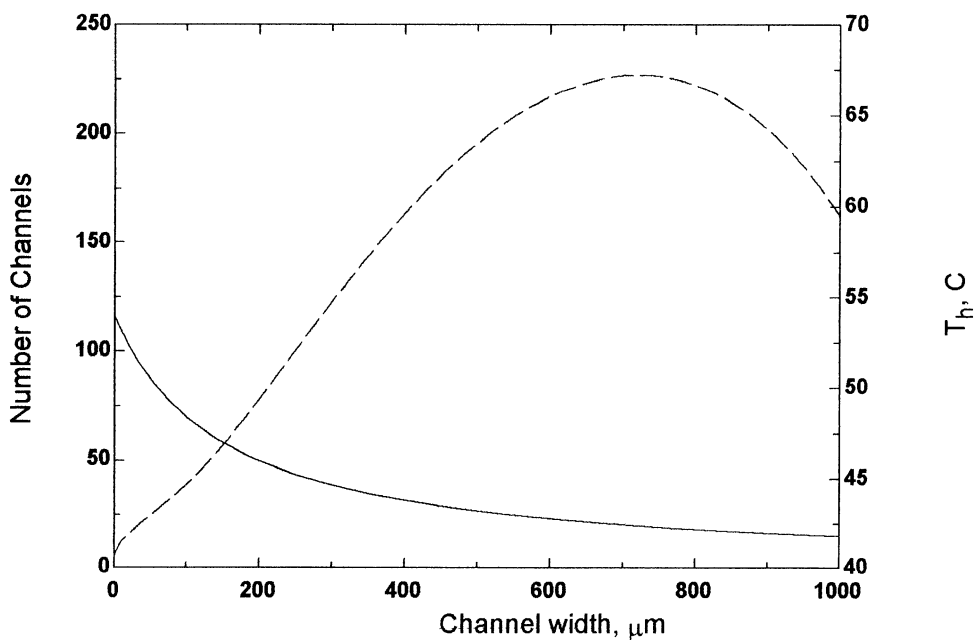


Figure 14: Channel Number & Heat Source Temperature vs. Channel Width, $w_{fin}=150 \mu\text{m}$

Case 4: Fin width, $w_{fin} = 200 \mu\text{m}$

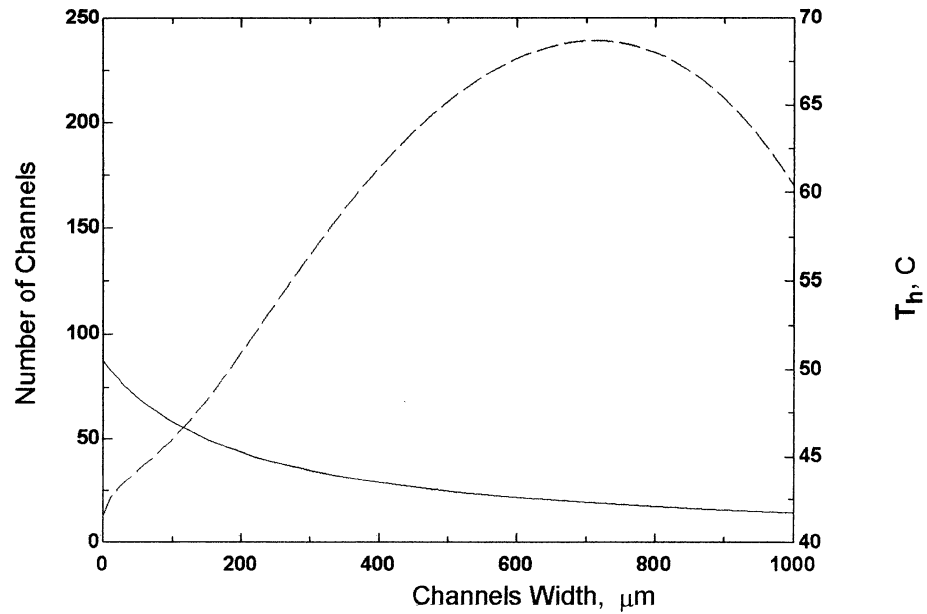


Figure 15: Channel Number & Heat Source Temperature vs. Channel Width, $w_{fin}=200 \mu\text{m}$

Case 5: Fin width, $w_{fin} = 250 \mu\text{m}$

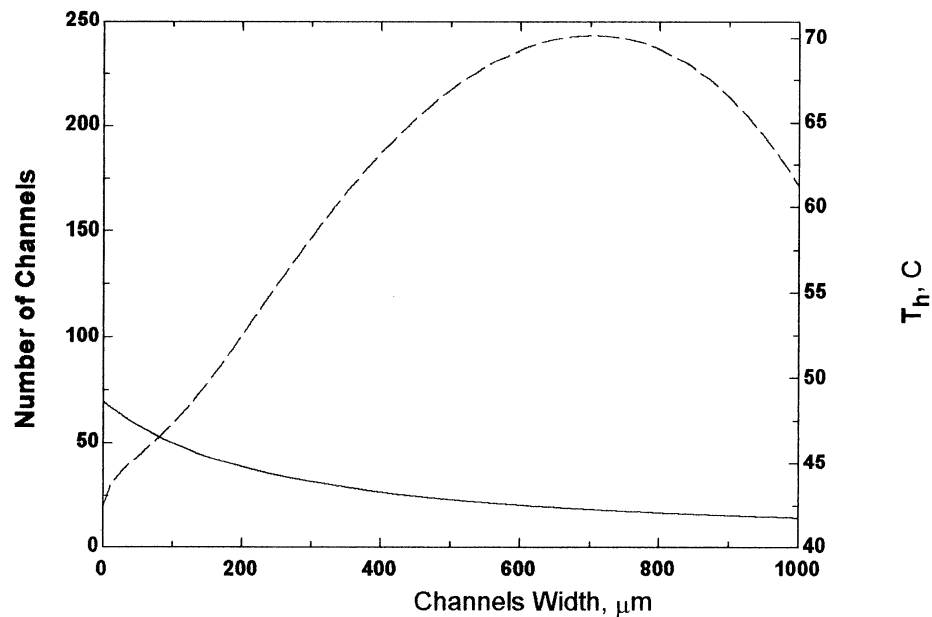


Figure 16: Channel Number & Heat Source Temperature vs. Channel Width, $w_{fin}=250 \mu\text{m}$

Looking back at these five cases, we can safely say that for all of them, a channel width above $500\mu\text{m}$ does not seem to be a good idea since the temperature is always going up and reaches a max at around $700\mu\text{m}$. Then beyond, $700\mu\text{m}$, the temperature drop but they are not interesting.

Secondly, the number of channel is also crucial. Indeed, a small channel width does guarantee a small heat source temperature but it is not as practical on the manufacturing point of view and narrow channel create structural problems. Then, the bigger the wall, the smaller the impact of the channel structure becomes.

Looking at each graph individually, one can realize the following remarks. For a fin width below $150\mu\text{m}$, the number of channel is too important and the structure of the channel might not be strong enough. For fin widths above $150\mu\text{m}$, and for a given channel width, the temperature of the heat Source becomes hotter.

Thus, in the purpose of our design, we decided to stick to the following parameters: fin width = $150\mu\text{m}$, Channel width = $250\mu\text{m}$, number of channel = 43.75, Foot-print = 3.5cm^2 , length = 2 cm, width = 1.75cm , channel height = $400\mu\text{m}$.

The temperature of the heat source is then $T_h = 52.2\text{C}$ and where the convection resistance represent 42 % of the total. One may notice that the Total resistance went up in value compared to the previous case at 100 cc/min. This is mainly due to a change in the flow.

	R_contact	R_bulk	R_cond	R_cont	R_conv	R_total
Resistance, K/W	0.00157	0.2053	0.007125	0.000534	0.1559	0.370429
Percentage, %	0.423833	55.42229	1.923448	0.144049	42.08638	100

Table 14: Percentage of resistance

4. Height influence

Figure 17 shows that the increase in the height lowers the temperature and the pressure drop. On the other hand, a high microchannel means a high heat sink, which really means a heavier cooling system than necessary. Also, wafer technology uses 500 μm quite a lot. Therefore, the height of 400 μm for the channel and the thickness of 100 μm at the bottom of the heat sink should be kept.

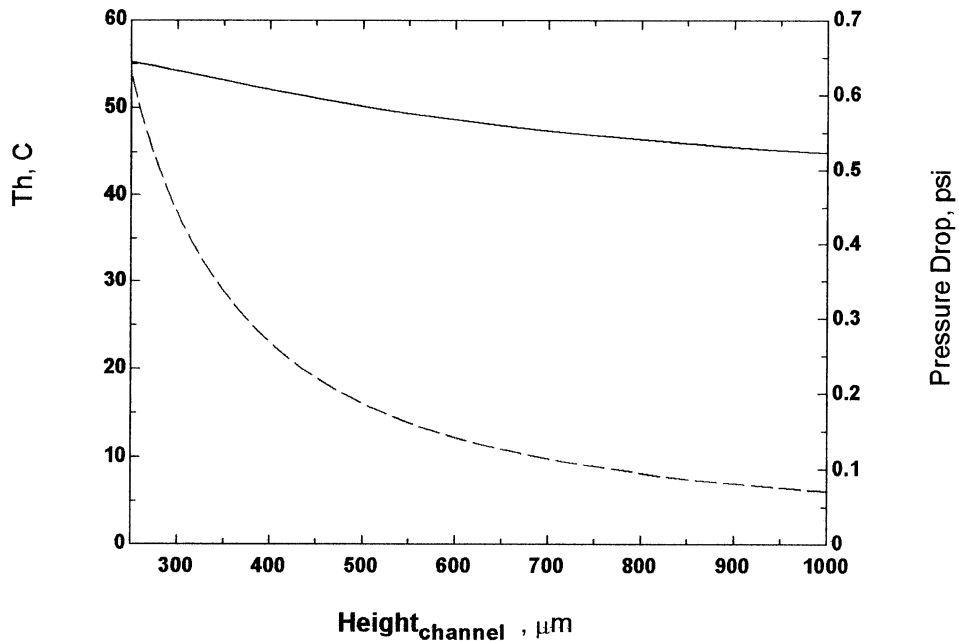


Figure 17: Temperature (C) & Pressure drop (dash line) vs. Channel Height

D. Results obtained using theoretical Microchannel Heat Sink Design

We had a heat flux of 25 W/cm^2 over a 3.7 cm^2 foot-print area. The goal was keep the maximum temperature in between 70 to 100C. Using Wei and Joshi's model we obtained this following optimized microchannel heat sink design, which gives a chip temperature of 52.2C, well below our intended goal.

Pure Copper, k=	401	W/mK
Channel width	250	μm
Fin Width (wall thickness)	150	μm
Channel height	400	μm
Length	2	Cm
Channel Number	43	
mass flow rate	70	cc/min
Heat Flux	25	W/cm^2
Total Resistance	0.37	C/W
Tin	20	C
Theater	52.2	C

Table 15: Results

V. Pump and Radiator Sizing

A. Pump Sizing

1. Pressure drop across the heat sink

Fluid flowing through the microchannel heat sink will experience a pressure drop, which are due to two sort of losses: Major loss and Minor loss. The same methodology is used in this case as in macro flow.

● Major Loss:

The friction factor for developing laminar flow in rectangular duct is provided in Dr. Wei and Dr. Joshi's model [6]. It is part of the Churchill-Usagi asymptotic model and is function of the channel aspect ratio, and the channel cross-section area. Once calculated, the friction factor can be used to find the major losses:

$$f = \frac{\left(\left[\left(\frac{3.44}{\sqrt{y^+}} \right)^2 \right] + \left(8 \times \sqrt{\pi} \times G(\alpha) \right)^2 \right)^{0.5}}{\text{Re}_{\sqrt{A_c}}}$$

$$y^+ = \frac{y}{\text{Re}_{\sqrt{A_c}} \times \sqrt{A_c}}$$

$$\text{Major Loss} = 4 \times f \times \frac{l_c}{d_h}$$

Major loss = 4 * friction factor *(Channel length / hydraulic Diameter)

● Minor Loss:

The minor loss is obtained with the following coefficient:

$K_{\text{entrance}} = 0.78$ due to Inward Projecting

$K_{\text{exit}} = 1.0$ due to exit of the flow.

$K_{\text{turn}} = 0.75$ due to standard 90° turn.

Therefore the pressure drop δp can be evaluated with the flow velocity V through the following equation:

$$\delta p = \frac{V^2}{2} \times (\text{Major Loss} + K_{\text{entrance}} + K_{\text{exit}} + 2 \times K_{\text{turn}})$$

From the configuration chosen above, the pressure drop across the microchannel heat sink was $\delta p = 0.268$ psi with a mass flow rate of 70cc/min.

The following graph shows how the pressure in psi and the heat source temperature are evolving with respect to the mass flow rate: a high flow rate guarantee a higher pressure and a lower temperature.

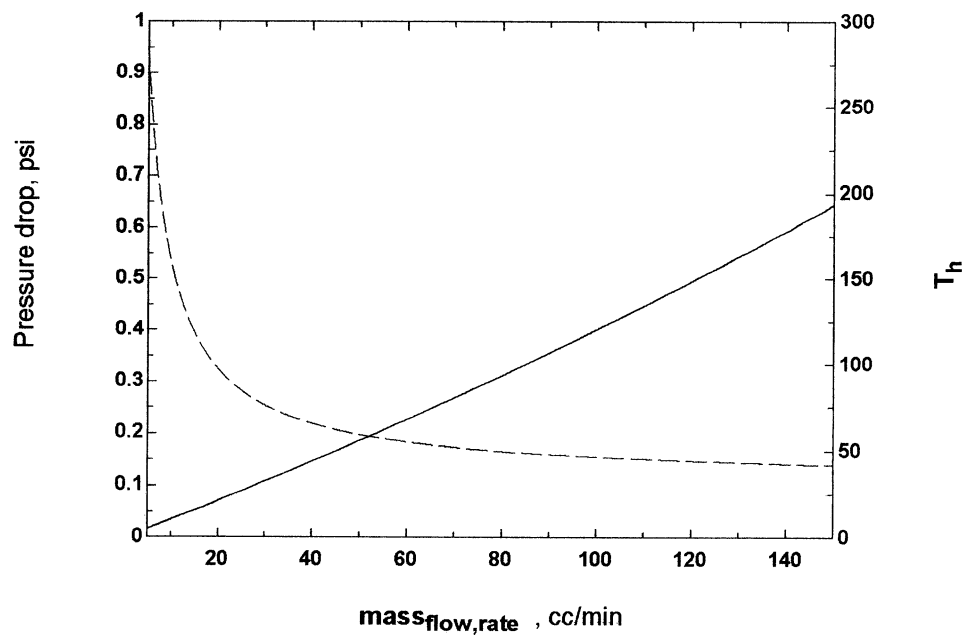


Figure 18: Pressure drop in psi and heat source Temperature (dash line) vs. mass flow rate

2. Different Pump Technology

A pump need to be size and chosen based on different parameters. First, it has to provide a constant flow rate of 70 cc/min as previously defined. Then, it had to overcome the pressure drops that will come from the heat sink (0.3psi) and from the radiator. Unfortunately, the radiator will not be entirely designed in this paper. In other words, to be able to pick a pump, one will have to know the pressure drop across the radiator. On the other hand, a suggestion of pump can be made.

Peristaltic pumps offer the range of flow rate needed for this project and a maximum pressure differential of a few dozen psi, which would probably be enough to cover the pressure drop across the radiator. These pumps also provides multi-channel system but have a high frequency in calibration. Their resistance to corrosion is very high, which is important since water is the working fluid. Other choice of pump are available in the literature and on the internet [16].

A piezo pump was also found to work for our project. The pump's mass flow rate provided by the pump can go as high as 120 cc/min. The pump can give a pressure of 1-4psi, which should be enough to cover the pressure drop from the heat sink and from the radiator. It sizes is only 1.125 in², which is perfect for the size of our satellite [17].

B. Radiator Sizing

The radiator is the piece of equipment of the satellite that will get rid of the wasted heat and that is connected directly down the flow from the microchannel heat sink. The following analysis is very simplistic. The absorbed heat is not accounted for

and therefore a more in-depth analysis is needed. In fact, this one has just be done to give the reader an idea of the size of the radiator. In the case that the spacecraft radiator is only radiating out the wasted heat from the high heat flux source and not absorbing any from space. Not counting for the loss of heat, it will have to radiate out

$$25 \text{ W/cm}^2 * 3.5 \text{ cm}^2 = 87.5 \text{ W}$$

The radiator has to verify the following equation:

$$Q = \epsilon * \sigma * \text{Area} * (T_2^4 - T_1^4)$$

Where $Q = 87.5 \text{ W}$.

$\epsilon =$ emissivity

$\sigma = 5.67\text{E-}8 \text{ W/m}^2 \cdot \text{K}^4$ Stefan-Boltzman Constant

Area = Area of the radiating surface in m^2

$T_2 = ((37.2+273)^4)$ Water temperature out of the heat sink

$T_1 = 0\text{K}$ Space temperature

Choosing a material whose emissivity is as close as 1 as possible, such as “Martin Black Velvet Paint” with $\epsilon = 0.94$ [8], the area then becomes:

$$\text{Area} = 0.177 \text{ m}^2$$

This area is to be considered to be very big compared to the total surface area of the spacecraft of 0.1m^2 . Two different designs could then be taken. First, a deployable radiator is attached to the main spacecraft and its surface area is 0.177m^2 . In this case, the deployable radiator might become a problem for the spacecraft dynamic and also for picking up heat from the environment. A second solution would be to have of the body of the satellite radiating the heat out. On the other hand, the radiator will take over the area reserved for the solar cells. This design issue of the radiator becomes crucial when the inter-dependence of each subsystem is taken into account.

VI. Reflection and Recommendations and Conclusion

In the first part of the project, a defined spacecraft in orbit with a high heat flux computer chip of $25\text{W}/\text{cm}^2$ was presented and a rough thermal design was done in order to see that a special thermal control subsystem is really needed. Concerning the Thermal Desktop model, improvements could be done such as looking at different operational modes. On the other hand, the primary purpose with this current model was reached. Indeed, the temperature of spacecraft becomes very hot when a high heat flux is applied and therefore it is important to design a proper thermal control.

In the second part of the project a cooling system using microchannel heat exchangers was developed. Two different analytical models were presented and studied and new model based on thermal resistances was created inspired by these two. The new model was benchmarked by previously published research based on analytical model or

experimental measurements. After the model was validated, it was used to design a system to remove a high heat flux of $25\text{W}/\text{cm}^2$. Only the foot-print area and the length of the microchannel were limited. The goal was to make sure that the temperature would not go over 70 to 100 Celsius degrees. The best solution for the analytical model was found.

In the last part of the project, the pressure drop across the heat sink was evaluated, and a possible pump was proposed to be integrated to the spacecraft. The design of a radiator in order to dump the wasted heat to space was also looked at. No final answer for the pump and the radiator were given since these must be developed for the specific application. Indeed the radiator must be fully designed before sizing the pump. Concerning the radiator, two schemes were suggested: an extended radiator and structural radiator. It is believed that the structural radiator will provide a better answer. Ultimately, a thorough model of the entire satellite with every subsystem is needed to see if a structural radiator could be doable.

Regarding the microchannel heat sink, a couple of recommendations can be made. Changing the working liquid in the microchannel would be interesting even though water seems to be doing quite of a good job for providing a high convection coefficient h but a low freezing point. Use of optimization algorithm could give more precise answers. On the other hand, with our model, the heat source temperature was well below $70\text{ }^{\circ}\text{C}$. To improve benchmarking, a computer model could be used. Although, CFD package do

not perform extremely well done to the micro level. Experiments should be run to verify the model that we have just presented.

References:

- [1] Baturkin, Volodymyr. *Micro-satellites Thermal Control-Concepts and components*. National Technical University of Ukraine, available at <<http://www.iaanet.org/symp/berlin/IAA-B4-0901.pdf>>.
- [2] Birur, Gajanana C, et al. *Micro/nano Spacecraft Thermal control using a MEMS-based pumped liquid cooling system*. Jet Propulsion Laboratory, California Institute of Technology, Science Applications International Corporation. Available: <<http://www.alumni.caltech.edu/~waniewsk/papers/waniewsk4.pdf>>.
- [3] Tabeling, Patrick. *Introduction à la microfluidique*. Paris: Edition Belin, 2003.
- [4] Gad-el-Hac, Mohamed, *The MEMS Handbook*. Boca Raton, Florida: CRC Press, 2002.
- [5] Nguyen, N.T., and S.T. Wereley. *Fundamentals and Application of Microfluidics*. Norwood: Artechhouse, 2003.
- [6] Wei, X., and Y. Joshi. "Optimization Study of Stacked Microchannel Heat Sink" *IEEE Transaction on Components and Packaging Technologies* Vol. 26, NO.1, March 2003, 55-61.
- [7] R.J. Phillips, "Micro-channel Heat sinks," in *Advances in Thermal Modeling of Electronic Components and Systems*, A. Bar-Cohen and A.D. Kraus, Eds., 1990, vol.2, pp.109-184.
- [8] David G. Gilmore. *Satellite Thermal Control Handbook*. El Segundo, California: The Aerospace Corporation Press, 1994.
- [9] Cal Poly San Luis Obispo cubesat team, 5 October 2004
http://cubesat.calpoly.edu/_new/workshop/index.html
- [10] Maynes, D., and B. Webb. "Fully-Developed Thermal Transport in Combined Pressure and Electro-Osmotically Driven flow in Microchannels" *Journal of Heat Transfer* 125 (2003): 889-895.
- [11] Fu, L., Lin, J., and R. Yang. "Analysis of electroosmotic flow with step change in zeta potential" *Journal of Colloid Interface science* 208 (2003): 266-275.
- [12] Frank P. Incropera. *Liquid Cooling of Electronic Devices by single phase convection*. New York, New York: Wiley, 1999.
- [13] Commercial website selling highly compound thermally conductive and adhesives, June 3rd, 2004 <http://www.arcticsilver.com/>

[14] M.M. Rahmann, "Measurements of Heat Transfer in Microchannel Heat Sink" Int. Comm. Heat Mass Transfer Vol. 27, NO. 4, 2000, pp. 495-506.

[15] Kandlikar, S. and W. Grande. "Evolution of Microchannel Flow Passages – Thermohydraulic Performance and Fabrication Technology" Proceedings of ASME International Mechanical Engineering Congress & Exposition. November 17-22, 2002, New Orleans, Louisiana.

[16] Commercial website selling micro systems, March 7th 2004 www.micropump.com

[17] Commercial website selling micro systems, October 20th 2004 www.partechinc.com